World Journal of Engineering and Technology, 2025, 13(3), 672-696
https://www.scirp.org/journal/wjet
ISSN Online: 2331-4249
ISSN Print: 2331-4222

Simulation and Estimation of CO_2 Emission and Concentration in the City of Douala: Case of Campus A, University of Douala-Cameroon

Ivan Aquigeh Newen[1*], Awa T. Achiri[1], Jean Bertrand Ngoulou Abomo[2], Alhadji Hisseine Issaka[3], Ayissi Zacharie[2], Bitondo Dieudonné[2]

[1]Faculty of Engineering and Technology, University of Buea, Buea, Cameroon
[2]Laboratory of Mechatronic, Energiatronic, and Sustainable Mobility, University of Douala, Douala, Cameroon
[3]Department of Physics, Cheihk Anta Diop University of Dakar, Dakar, Senegal
Email: *ivanaquigeh@gmail.com, awaterence9@gmail.com, jngoulouabomo@yahoo.fr, elhadj hissen@yahoo.fr, gresidd.ufdsi@gmail.com, bitondodieudonne@yahoo.fr

How to cite this paper: Newen, I.A., Achiri, A.T., Abomo, J.B.N., Issaka, A.H., Zacharie, A. and Dieudonné, B. (2025) Simulation and Estimation of CO_2 Emission and Concentration in the City of Douala: Case of Campus A, University of Douala-Cameroon. *World Journal of Engineering and Technology*, **13**, 672-696.
https://doi.org/10.4236/wjet.2025.133042

Received: July 12, 2025
Accepted: August 22, 2025
Published: August 25, 2025

Abstract

Douala-Cameroon is a growing city with huge number of cars and motorcycles plying the roads, especially during rush hours. These automobiles emit exhaust gases, leading to atmospheric pollution. By simulating and measuring the concentration of carbon dioxide (CO_2) gives a view of the quality of air consume around and within the University of Douala main campus. The study involved both experimental and numerical models developed for atmospheric pollution dispersion in street canyons. A computational fluid dynamics (CFD) simulating software, FLUENT version 6.3.26 in combination with a grid generating preprocessor GAMBIT version 2.4.6 and a post processor Tecplot version 08 for animation and visualization of results were employed for simulations. The computational domain is discretized with unstructured triangular cells. Measurements were done during the morning and evening rush hours, using the gas tester, KIMO-KIGAZ 700 (060322). For both simulated and measured data, the model named Campus led to the maximum concentrations, while the model named BATI led to the minimum concentrations (3.09 and 1.35), (2.53 and 0.34) respectively. This high concentration is proportional to the number of buildings per model and it is advised that during rush hours occupants of this stretch of buildings should take necessary majors to avoid developing respiratory health challenges. Average total CO_2 emission is estimated at 143.2 kg/rush period, with motorcycles contributing highest (75.8 kg/2h) and cars (67.4 kg/2h). The results indicate that, motorcycles significantly affect air quality in urban cities.

Keywords

Ubanair Quality, Sustainability, Exhaust Emission, Pollutant Dispersion, Urban Traffic, Concentration, Measurement

1. Introduction

Air quality remains a key aspect in city sustainability. Despite the efforts made to improve on air quality in cities, urbanization and huge industrial and transportation activities, emissions keep rising and pollution follows. The air pollutants in the urban air we breathe are a public health problem. It is of interest to improve air quality. To do this effectively, it requires an understanding of the sources and how the pollutants spread. Measurements and modelling provides a good knowledge base to enable actions towards achieving cleaner air. Many factors do influence urban air quality, for example, background concentrations and sources of local emission vary across the country. Meteorology and building set-outs can also impact pollution concentrations largely [1].

Douala is the commercial and economic capital of Cameroon and the entire CEMAC region comprising Gabon, Congo, Chad, Equatorial Guinea, Central African Republic and Cameroon. The population of Douala has grown from 1.9 million in 2005 to 5,066,000 in 2023 [2], making it a poll of intense economic, social and industrial activities impacting the environment. Consequently, the air quality and other sustainability issues needs to be monitored and evaluated.

Apart from industrial emissions, automotive vehicles constitute a major source of atmospheric pollution. Several studies have investigated and provide data on emissions from automobile engines, their diffusion into the atmosphere, and their effects on humans. Carbon dioxide even though not toxic, causes the greenhouse effect. *i.e.* it causes global warming (by depletion of the ozone layer) and exposes humans to ultra-violet rays from the sun, Volkswagen [3]. Projections indicate that by 2030 about 60% of the world's population will be living in urban arears. Due to this growth, the urban ecosystems will strongly be affected negative due to increase in energy demands, leading to emission of air pollutants. Some of the major sources of air pollution are the transport sector, heating of buildings and industrial processes. International bodies concluded that air pollution constitutes one of the major problems in urban areas, causing several respiratory and circulatory system diseases leading to several premature deaths per year worldwide. That climate changes are caused by an increase in the concentration of carbon dioxide, estimating that after the emissions stop, it would take about 1,000 years to return to the previous state, and the levels of average concentrations of CO_2 in the atmosphere would be likely to increase from the current 385 ppm to 450 - 600 ppm. Such levels of carbon dioxide may speed up photosynthesis, and thus leading to climate changes and adverse effects on humans, animals and vegetation [4]-[6]. A number of studies have explored ways for accurate measurement and monitor-

ing of CO_2 dispersion with different methods, such as: the use of street canyons, the eddy covariance (EC) method, which analyze changes in CO_2 concentrations and try to determine their impact on the functioning of users of the area, evaluating the shape of a tree's crown and its impact on CO_2 dispersion from transportation, Operational Street Pollution Model (OSPM), facilitating the monitoring of exposure to pollutants by human, prioritizing industrial activities and vehicle types, to reduce odours, smoke and soiling from emissions. To reduce emissions, transportation in the city needs to largely be in the form of walking and cycling, supplemented by an attractive and well-functioning public transport system. Therefore, these traffic types need to be given more space in cities and in urban planning. Walking and cycling have great potential to replace short car trips in our urban areas [4]-[8]. Increasing industrialisation in the 19th century led to a significant increase in coal consumption and with it, higher emissions. International collaboration regarding both measurements and emissions reduction began when air pollutants were recognised as a major regional problem in the late 1960s. Local-scale dispersion models can describe the effects of buildings on ventilation. These models provide valuable insights for urban planning and air quality monitoring, but they require high-quality input data to provide reliable results. Particles of condensed carbonaceous material are emitted mainly by diesel and motor vehicles with inadequate maintenance [9].

Furthermore, studies have shown that, air exchange between street level and the atmospheric wind above the roof level is limited inside the street canyon, and the near ground vehicular pollutant emissions are not effectively diluted and removed, which considerably deteriorates the pedestrian level air quality in the street canyon and imposes harmful impacts on the health of the city population. The primary methods to study the flow fields and pollutant dispersion within the street canyon include field measurements, laboratory physical experiments, and numerical simulation. Field measurements are limited by their low spatial resolution, high cost, and uncontrollable meteorological conditions. Physical experiments provide data only for a few number of discrete measurement points [10].

There are three main approaches in monitoring pollutant dispersion. The number of field studies seems scarce compared to wind/water tunnel or CFD studies (in only 28 studies field measurements were used, in contrast to 137 studies which used CFD or a wind/water tunnel setup). However, due to the complexity and unresolved issues of CFD, it is not a feasible tool to be used by urban planners [11]. This indicates the necessity for a closer collaboration between engineering sciences and urban planning. This indicates the necessity of more field studies, to test and complement the mere computational studies. A number of studies have developped models using the different approaches. The combined analysis of measurement and modeling showed the importance of reliable field measurements and CFD simulations with a high spatial resolution to assess transport mechanisms in urban areas. Gartmann *et al.* [12], described the numerical approach and the com-

parison of CFD CO_2 results with field measurement data in a real city geometry, using basic guidelines for CFD calculations in urban areas. Based on these guidelines, a sensitivity study was first conducted to determine the numerical parameters that influence the calculations. An appropriate time-average period for the Reynolds decomposition in the measurement data had to be defined for the comparison of RANS models with field measurements [12]. Urban-scale traffic pollution dispersion model is developed considering street distribution, canyon geometry, background meteorology, traffic assignment, traffic emissions and air pollutant dispersion.

Bjorkegren *et al.* [4] found that an increase in building height leads to heavier pollution inside canyons and lower pollution outside canyons at pedestrian level, resulting in higher domain-averaged concentrations over the area. In addition, canyons with highly even or highly uneven building heights on each side of the street tend to lower the urban-scale air pollution concentrations at pedestrian level. Further, increasing street widths tends to lead to lower pollutant concentrations by reducing emissions and enhancing ventilation simultaneously. The results indicate that canyon geometry strongly influences human exposure to traffic pollutants in the populated urban area. Calculation of residence and exposure times for an idealized street canyon in the skimming-flow region and a deep street canyon within a realistic urban area using large-eddy simulation and a Lagrangian particle model [13]-[15]. Effects of the wind flow velocity on the air flow and the air pollution dispersion in a street canyon with Skytrain, using finite element method, and obtaining the governing equations of air pollutants and air flow in this study area are the convection-diffusion equations of species concentration and the Reynolds-averaged Navier-Stokes (RANS) equations of compressible turbulent flow, respectively. COMSOL Multiphysics Modelling software. The model obtained can depict the airflows and dispersion patterns for different wind conditions [16]. Evaluations on the ability of Reyonds stress model (RSM) to predict dispersion of carbon dioxide (CO_2) cloud, are done using CFD simulation using Fluent and statistical performance indicators. The results revealed that stress-ω model exhibits different capacities in flat terrain and urban terrain. Specifically, stress-ω model can present better results than SST k-ω model in flat terrain, and it performs better in the far-field region than in the near-field region. Although SST k-ω model can describe CO2 dispersion more accurately in urban terrain, the concentration distribution reproduced by stress-ω model is still within acceptable range [17]. Three k-ε turbulence models, including the standard k-ε model, the renormalization group (RNG) k-ε model [9], and the realizable k-ε model were employed and validated against two independent wind tunnel experiments of street canyon. Although there are no clear differences among diverse categories, models might be classified into groups according to their physical or mathematical principles (e.g. box, Gaussian, regression, CFD) or their level of complexity (e.g. screening, semi-empirical, numerical). CFD modelling is a specific term used to describe the quantitative and qualitative evaluation of systems involving fluid

flow, heat transfer and associated phenomena (e.g. chemical reactions, diffusion etc.) using computer-based numerical methods. Modelling helps evaluate the correlation between the pollutants sources and their effects on ambient air quality [18]. Mobile monitoring (field measurement) and computational fluid dynamics (CFD) modeling, indicated that, high emitting vehicles (HEVs) are deterministically responsible for poor air quality in the street canyon, suggesting that the number of HEVs and street-canyon ventilation, especially near a signalized intersection, need to be controlled to mitigate poor air quality in a central business district of a megacity [19]. Besides, pollutants in street canyons have a significant influence on IAQ. Making clear that in addition to forced convection that is directly caused by air flow, natural convection caused by temperature difference and the gravity effect of pollutants are also driving forces to promote pollutant dispersion [20]. Ketzel *et al.* [21], equally used OSPM vs Measurements and showed that OSPM calculations were in good agreement with the measurements for seven out of nine street sections.

On the global scale, the road traffic is known to be the major contributor to the anthropogenic emissions of the "greenhouse" gas Carbon Dioxide (CO_2) and it is expected that these emissions will continue to increase with the steadily increasing amount of traffic. Potentially, the emissions of road wear particles could even be greater from EVs, as they are generally heavier due to their batteries [22] [23]. Gregory *et al.* [24], suggested new solutions to air pollution challenges, amongst which are: Cultivating a safer and more attractive environment for cycling, Electrification of public vehicles, Transforming the private vehicle fleet (changing from diesel to gasoline will reduce Nox but will promote CO_2 production, electrification is the best solution), and ecological interventions. Increasing canyon width reduced the residence time of pollutant and reduces ingress. Flat roofs for both ratios drew CO_2 to the leeward side of the building due to negative pressures. However pitched roofs created more complex systems that reduced contaminant in the canyon due to unsteady vortices. This may indicate a decrease in vertical exchange due to intermittent turbulent structures which maintain overall mass transfer with the air above [25].

Flow characteristics of vehicle exhaust gases have been modelled [26], with the discrepancy taken care of by introducing a flow coefficient. For passages of the same shape but of different size, it has been shown that the flow coefficient is a function of the Reynolds and the Mach numbers. The structure of the urban atmospheric boundary layer is modeled as a multi-layer air flow, where by airflow reaches the city; the wind profile is adjusted to its roughness conditions. An initial boundary layer forms above the city, which displaces the outer boundary layer of the approach wind profile [27]. Horizontal movement of the atmosphere (the horizontal component of winds) is driven mostly by uneven heating of the earth's surface and modified by the effect of the earth's rotation (coriolis force) and the influence of the ground and the sea. Most vertical motions in the atmosphere are caused by changes in air density. Any parcel of air that is less dense than the air

that surrounds it will rise by buoyancy, and any parcel denser than the surrounding air will sink by negative buoyancy [28].

The physics that govern the geophysical flow of ordinary fluids (air and water) is codified by the conservation laws of classical mechanics: conservation of mass, and conservation of (linear) momentum, angular momentum and energy. These conservation laws are applied to the analysis of fluid flow by first of all erecting a coordinate system that is suitable for describing a fluid flow, and followed by deriving the mathematical form of the conservation laws that correspond to the system. This coordinate system will represent the motion and properties of a fluid at every point in a domain (the space occupied by the material), as if the fluid material was a smoothly varying continuum. These laws are found in the Lagrangian, Eulerian, and the Navier–Stokes fluid flow theories [29]. One practical fluid flow theory applied to physical phenomena are provided by SUHAS V. PATANKAR [30], he developed a practical approach for velocity field problems and the appropriate Numerical methods used in solving such problems. Patankar succeeded in removing the difficulties faced by standard F.E.M. by using a F.E.M based on a control volume.

Previous studies elaborated on a number of schemes for solving fluid dynamic problems numerically (RANS, k-ϵ, k-ω, LES). Experimental and numerical models developed for atmospheric pollution dispersion in street canyons [31] [32]. Within the scope of an experimental method (Environmental Wind tunnels) Plate and Kasner-Klein [33] [34] developed mathematical models describing traffic induced pollution in cities. Ibrahim *et al.* [32] presented variations in pollutant concentration within street canyons using a numerical approach. A study of vehicle exhaust dispersion within different street canyons models in an urban ventilated by cross-wind is conducted within this work, to investigate how pollution dispersion is affected by wind speed, building height to width ratios, street and building geometries, and canyon street number. For all cases, cars exhaust was represented by a line source emitting CO_2 and pollution dispersion was studied in two and three dimensions, airflow and the street canyons were assumed thermally isolated. The FLUENT Computational Fluid Dynamics (CFD) software package was used with a standard k-ε, RNG k-ε and sstk-ω turbulence models to simulate different street canyon models.

Central to the discipline of atmospheric pollution are the theories describing fluid flow by Lagrange, Euler, Navier-stokes, Patankar *et al.*, and others, which have brought to light the facts that physical phenomena are described by differential equations through which the various parameters are related by the conservation laws and can be calculated by means of numerical tools. This study makes use of the above theories as applied to atmospheric pollution dispersions. Viscous-k-ε model is used as it is more advantageous, compared to other models. Peculiar to this study, is the measuring scheme and the presentation of findings. This is with respect to the growing number of vehicles in the city of Douala as a whole and around the university environs in particular.

2. Materials and Methods

This study describes the numerical approach and the comparison of CFD CO_2 results with field measurement data in a real city geometry, Using basic guidelines for CFD calculations in urban areas from the literature. A CFD simulating software, FLUENT version 6.3.26 is adopted, in combination with a grid generating preprocessor GAMBIT version 2.4.6 and a post processor Tecplot version 08 for animation and visualization of results. The computational domain is discretized with unstructured triangular cells. The grid density is made denser near the walls to improve accuracy and is less denser away from the walls to optimize computational time and memory constraints.

FLUENT is constituted with modules that solve the species transport equation, the equations for the conservation of Mass, Momentum and Energy. The Turbulence models and the species transport equations derived from the conservation of Momentum are used to calculate the flow parameters such as the turbulent kinetic energy, the length scales, the dissipation rates, the turbulent velocity and the chemical and transport properties of the pollutants.

Existing models are presented below to enable the choosing of an appropriate model.

2.1. The General Differential Equation for Velocity Field Problems

$$\frac{\partial}{\partial t}(\rho\phi)+\operatorname{div}(\rho u\phi)=\operatorname{div}(\Gamma_l \operatorname{grad}\phi)+S_\phi \tag{1}$$

The four terms in the general differential Equation (1) are the unsteady term, the convection term, the diffusion term and the source term respectively. The dependent variable ϕ can stand for a variety of different quantities, such as the mass fraction of a chemical species, the enthalpy or the temperature, a velocity component, the turbulence kinetic energy, or a turbulence length scale.

Accordingly, for each of these variables, an approximate meaning will have to be given to the diffusion coefficient Γ. and the source term *S*.

Note:

Not all diffusion fluxes are governed by the gradient of the relevant variable. The use of $\operatorname{div}(\Gamma\operatorname{grad}\phi)$ as diffusion term does not, however, limit the general ϕ equation to gradient driven diffusion processes. In fact, Γ can even be set to zero.

The flow field should satisfy the mass conservation or the continuity equation;

$$\frac{\partial\rho}{\partial t}+\operatorname{div}(\rho u)=0 \tag{2}$$

The Cartesian-tensor form of Equation (1) and Equation (2) are:

$$\frac{\partial}{\partial t}(\rho\phi)+\frac{\partial}{\partial x_j}(\rho u_j\phi)=\frac{\partial}{\partial x_j}\left(\Gamma_{\cdot}\frac{\partial\phi}{\partial x_j}\right)+S_{\cdot} \tag{2a}$$

$$\frac{\partial\rho}{\partial t}+\frac{\partial}{\partial x_j}(\rho u_j)=0 \tag{2b}$$

j can take the values 1, 2, 3. *i.e.*;

$$\frac{\partial}{\partial x_j}\left(\Gamma.\frac{\partial \phi}{\partial x_j}\right)=\frac{\partial}{\partial x_1}\left(\Gamma.\frac{\partial \phi}{\partial x_1}\right)+\frac{\partial}{\partial x_2}\left(\Gamma.\frac{\partial \phi}{\partial x_2}\right)+\frac{\partial}{\partial x_3}\left(\Gamma.\frac{\partial \phi}{\partial x_3}\right)$$

$\frac{\partial}{\partial x_1}\left(\Gamma.\frac{\partial \phi}{\partial x_1}\right)+\frac{\partial}{\partial x_2}\left(\Gamma.\frac{\partial \phi}{\partial x_2}\right)+\frac{\partial}{\partial x_3}\left(\Gamma.\frac{\partial \phi}{\partial x_3}\right)=0$; is the Helmhorltz equation for scalar fields

$$\frac{\partial}{\partial x_j}\left(\rho u_j\right)=\frac{\partial}{\partial x_1}\left(\rho u_1\right)+\frac{\partial}{\partial x_2}\left(\rho u_2\right)+\frac{\partial}{\partial x_3}\left(\rho u_3\right)$$

The recognition that all the relevant differential equations for heat, mass transfer, fluid flow, turbulence and related phenomena can be thought of as particular cases of the general ϕ equation is an important time-saving step. Since it can be repeatedly used for different meaning of ϕ along with appropriate expressions for Γ and *S*, and of course with appropriate initial and boundary conditions. The concept of the general ϕ equation enables us to formulate a general Numerical method and to prepare general purpose computer programs.

2.1.1. Calculation of the Flow Field

The velocity components are governed by the momentum equations. This momentum equations are special cases of the general differential equation for ϕ where ϕ and Γ and other parameters are replaced; *i.e.* $\phi = u$, $\Gamma = \mu$ and so on.

The difficulty in the calculation of the velocity field lies in the unknown pressure field. The pressure gradient forms part of the source term for a momentum equation. If the pressure field is given, the momentum equation becomes easy to solve.

2.1.2. Convection and Diffusion Problems

From the general differential equation for velocity field problems:

$$\frac{\partial}{\partial t}\left(\rho\phi\right)+\frac{\partial}{\partial x_j}\left(\rho u_j\phi\right)=\frac{\partial}{\partial x_j}\left(\Gamma.\frac{\partial \phi}{\partial x_j}\right)+S.$$

Since the flow field must satisfy the continuity equation:

$$\frac{\partial \rho}{\partial t}+\frac{\partial}{\partial x_j}\left(\rho u_j\right)=0$$

The general differential equation becomes:

$$\rho\frac{\partial \phi}{\partial t}+\rho u_j\frac{\partial \phi}{\partial x_j}=\frac{\partial}{\partial x_j}\left(\Gamma.\frac{\partial \phi}{\partial x_j}\right)+S. \tag{3}$$

ϕ can be: a chemical species, diffusion flux, heat flux, viscous stress, etc.

2.2. Numerical Solutions to Physical Phenomena

2.2.1. Methods of Deriving the Discretization Equations

For a given differential equation, the required discretization equation can be derived in many ways. Here, we shall outline a few common methods and then in-

dicate a preference:

- Taylor-series formulation
- Variational formulation
- Method of weighted residuals with special cases as; Galerkin method, control volume formulation.

The control volume formulation satisfies the integral conservation of quantities such as mass, momentum, and energy over any group of control volumes and of course, over the whole calculation domain.

2.2.2. A Control Volume Based Finite Element Method

The difficulties faced by standard F.E.M. were removed by using a F.E.M based on a control volume [30].

Steps:

1) For the triangular grid the dependent variables are calculated for grid points that lie at the vertices of the triangles. The discretization equations are formed by the control volume method (*i.e.* the differential equation is integrated over the typical control volume as shown below). The control volumes are constructed by joining the centroid of each triangle to the midpoints of the sides of that triangle (**Figure 1**). The discretization equation is formed by adding the contribution of these elements to the integral conservation for the control volume.

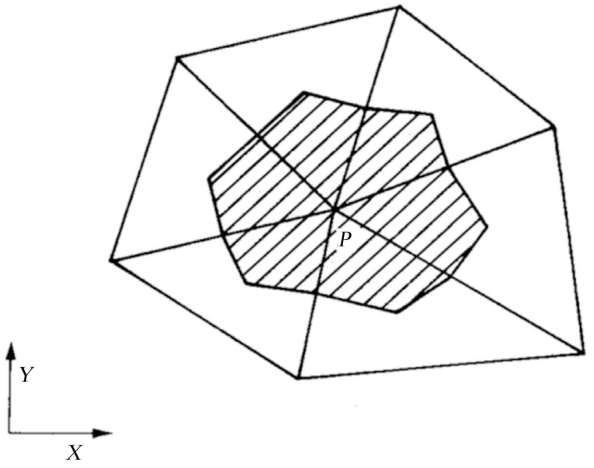

Figure 1. Control volume for the triangular grid [30].

2) The shape function describing the variation of ϕ over an element is needed to calculate the flux across the control-volume faces that fall within the element. The standard shape function for the triangular element is;

$$\Phi = a + bx + cy \tag{4}$$

This gives birth to difficulty; so, the above shape function is unacceptable. The alternative proposed by Baliga and Patankar [30], is the shape function:

$$\Phi = A + B\exp\frac{\rho uX}{\Gamma} + CY \tag{5}$$

u: is the resultant velocity in the element.

X: is the coordinate pointing in the direction of the resultant velocity.

Y is the direction normal to X.

A, B, and C are found in terms of the three values of Φ at the vertices of the triangle.

For low peclet numbers Equation (5) boils down to Equation (4) which is the appropriate shape function for conduction problems.

It is through Equation (5) that the spirit of the exponential scheme has been introduced into the finite element method.

Note: F.E.M. based on Equation (5) produces much less false diffusion than does other formulations.

3) The issue of the staggered grid is handled by calculating the pressure on a grid that is different from the grid used for all the other variables. The pressure is calculated at the vertices of "macrotriangles" which are shown by small circles. Figure 2, shows each macrotriangle divided into four subtriangles. The subtriangles form the grid for the velocity components and all other variables except pressure.

Note: peclet number is directly proportional to the distance between grid points.

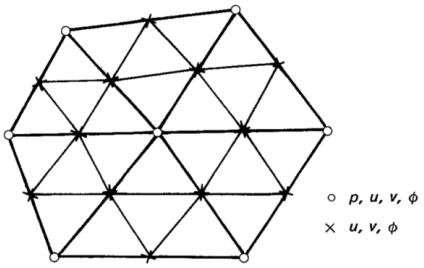

Figure 2. Macrotriangles and subtriangles [30].

4) A sequential solution algorithm is formulated. The pressure equation and the pressure-correction equations are derived from the continuity equation written for a control volume defined by the macrotriangle.

The control volume based-F.E.M. represents a logical and effective extension of discretization.

2.3. Wind Tunnel Modeling of Traffic Induced Pollution in Cities

Within the scope of an experimental method (Environmental Wind tunnels) [33] [34], have developed mathematical models describing traffic induced pollution in cities.

2.3.1. Neutral Wind Profiles for Urban Areas

- **Power-law equation**

$$\frac{u(z)}{u_{ref}} = \left(\frac{z}{z_{ref}}\right)^{\alpha} \tag{6}$$

It expresses the wind velocity profile, for modest (4 m/s and up) wind speed conditions.

it is the prerequisite for E.W.T modelling [27].

➢ **Logarithmic law**

$$\frac{u}{u_*} = \frac{1}{k} \ln \frac{z - d_0}{z_0} \tag{7}$$

$$u_* = \sqrt{\frac{\tau}{\rho}}$$

Note: d_0 and z_0 are determined by the building configurations.

The earliest ones [33], assumed a relationship between d_0 and z_0 and average roughness height H such as:

$$z_0 = 0.15H \text{ , and } \quad d_0 = 0.85H \tag{8}$$

Equation (7) was solved, at a height z 10 to 15 times above z_0 but within the logarithm limits and came out with the expression:

$$u_* = \frac{k \cdot u(h)}{\ln\left[(h - d_0)/z_0\right]} \tag{9}$$

Two parameters (coefficients) for the classification of roughness in terms of building arrangements were found and defined as:

$\lambda_{ar} = \Sigma$ of areas covered by buildings/total urban area

$\lambda_{fa} = \Sigma$ of average building areas normal to the wind/total urban area

$$z_0 = 0.25H \cdot \lambda_{ar} \tag{10}$$

2.3.2. Modelling of Moving Traffic

$$\frac{P_{Tm}}{P_{Wm}} = \frac{P_{Tn}}{P_{Wn}} \tag{11}$$

m : model; n : full size

P_T : Energy caused by moving traffic

P_W : Energy caused by wind

P_T is given per unit street length, by the expression:

$$P_T \frac{\rho C_{DT} A_{T.} n_{T.} u_T^3}{B \cdot H} \tag{12}$$

where ρ is the density of air, C_{DT} is the drag coefficient of the (average) vehicle, A_T is the frontal area, and u_T its velocity. $n_{T.}$ is the number of vehicles per unit length.

For P_W they obtained:

$$P_W = \tau \frac{\Delta u}{\Delta z} \approx \frac{\rho u_*^2}{H} u(H) = \frac{\rho \cdot c_{fh} \cdot u_{ref}^3}{H} \tag{13}$$

where the shear velocity $u_* = \sqrt{c_{fh.} u_{ref}}$ has been expressed through the friction coefficient $c_{fh.}$ consequently, eq. (11) requires that the ratio (the modelling law):

$P_T = \dfrac{C_{DI} A_{T.} n_{T.}}{c_f \cdot B} \dfrac{u_T^3}{u_{ref}^3}$ must be the same in model and prototype.

2.3.3. Wind Tunnel Modelling of Diffusion in a City Complex

Here the model considers pollution from different sources (traffic, point sources, etc.). If the quantity to be determined is a concentration from a line source of traffic, then the tunnel experiment is conducted with an emission rate E_m per unit length of the line source, which yields the dimensionless concentrations:

$$C^*\left(\alpha, u_{ref}\right) = \frac{c_m\left(\alpha, u_{ref}\right)}{E_m} u_{mref} \cdot L_m \tag{14}$$

$c_m\left(\alpha, u_{ref}\right)$: measured concentration;

u_{mref}: reference velocity for the model;

L_m: characteristic length.

Model emission E_m has the dimension $c_o \cdot q$, where c_o is the concentration in the emitted gas flow rate q per unit length, which is selected to yield concentration c_m in the model, which can be measured conveniently with the available analysis equipment.

2.3.4. Application of Wind Tunnel Studies to Urban Pollution from Traffic

A basic study for street canyons is shown in Figure 3, with the following considerations [34]:

- Line source emitting continuous discharge of tracer gas
- The variable to be studied is the geometry of the building rows, starting with a reference case of buildings of quadratic cross sections of width B and height H.

($B_1/H = 1$; $B_2/H = 1$) placed at a distance of SI ($SI/H = 1$) apart.

The wind direction is perpendicular to the building rows, as shown below.

- The first step is to determine the uniformity of the line source, by using a design of Meroney *et al.* [31].

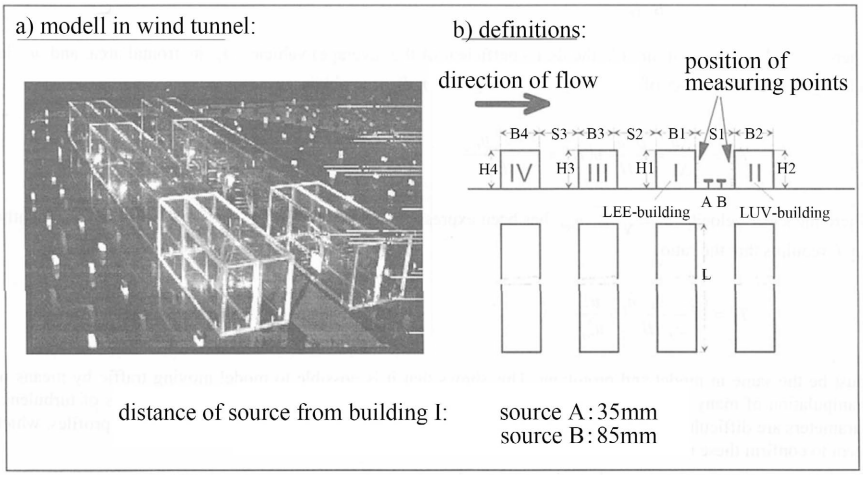

Figure 3. Concentrations in street canyons: Cases studied [34].

2.3.5. Modeling of Air Pollutant Dispersion in Street Canyons in Cross-Wind

The relative speed is corrected by $\sqrt[3]{a}$. The important combination $\sqrt[3]{a \cdot \frac{v}{u}}$ postulated as factor in the modelling law above produced correct scaling of wind tunnel data (a represents a scaling factor for the traffic density). Further, the result show that the effect of the combination $\sqrt[3]{a \cdot \frac{v}{u}}$ is linear, *i.e.*:

$$c^{**}\left(\alpha, u_{ref}, v\right) = c^{*}\left(x, y, z, \alpha\right)\left[1 - \phi \cdot a^{1/3}\frac{v}{u}\right] \tag{15}$$

where $c^{*}\left(x, y, z, \alpha\right) = \frac{C\left(x, y, z, \alpha\right)}{E} L \cdot u_{ref}$ is the dimensionless concentration for the case without moving vehicles ($v = 0$) calculated in the usual way by means of eq. (14). Consequently the effect of traffic amounts to a reduction of the velocity by a term $\phi \cdot a^{1/3} \cdot v$ in calculating the effect of moving traffic.

2.3.6. 2-D physical Modeling of Pollutant Dispersion in Street Canyons

Ibrahim *et al.* [32] have presented variations in pollutant concentration within street canyons using a numerical approach. A study of vehicle exhaust dispersion within different street canyons models in an urban ventilated by cross-wind is conducted at this work to investigate how pollution dispersion is affected by wind speed, building height to width ratios, street and building geometries, and canyon street number. For all cases, cars exhaust was represented by a line source emitting CO_2 and pollution dispersion was studied in two and three dimensions, airflow and the street canyons were assumed thermally isolated. The FLUENT Computational Fluid Dynamics (CFD) software package was used with a standard k-ε, RNG k-ε and sstk-ω turbulence models to simulate different street canyon models.

The main parameter to be calculated is the non dimensionless parameter

$$K = \left(CU_{\infty}h\right) \Big/ \left(\dot{Q}_{c_{02}} \Big/ l\right) \tag{16}$$

C is the volume fraction of pollutant, h is the building height, and $\dot{Q}_{c_{02}} \Big/ l$ is the emission source strength per unit length. For outlet flow, an outflow boundary condition was assumed.

For this study, **Figure 4** shows the contour of the simulated concentration as is displayed from Fluent showing the flow pattern of CO_2 in the atmosphere and around the buildings in the case with an obstacle. Here we are presenting the dimensionless concentration and not the molar concentration as above.

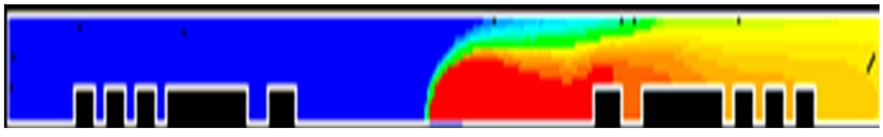

Figure 4. Simulation contour display of dimensionless concentration (k) of CO_2 (Wind speed, 1 m/s).

Similarly, Figure 5 gives a contour for a wind speed of 0.8 m/s, as simulated in this study. The dimensionless concentration displayed from Fluent showing the flow pattern of CO_2 in the atmosphere and around the buildings in the case with an obstacle. Here we are presenting the dimensionless concentration with a velocity of 0.8 m/s for the gases.

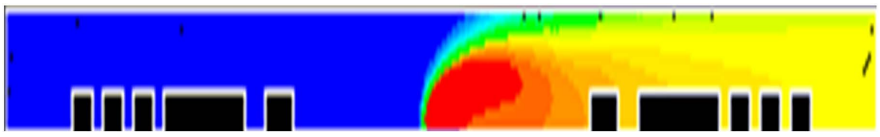

Figure 5. Simulation contour display of dimensionless concentration (k) of CO_2 (wind speed, 0.8 m/s).

Furthermore, Figure 6 displays the contour for the values for a wind speed of 0.5 m/s, simulated in Fluent.

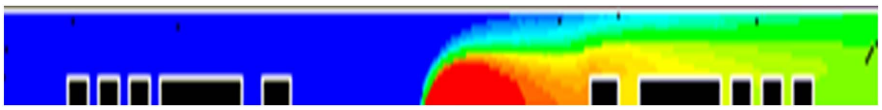

Figure 6. Simulation contour display of dimensionless concentration (K) of CO_2 (Wind speed, 0.5 m/s).

Another wind speed of interest is 0.1 m/s. Shown in Figure 7, its contour of the simulated concentration is displayed from Fluent, showing the flow pattern of CO_2 in the atmosphere and around the buildings.

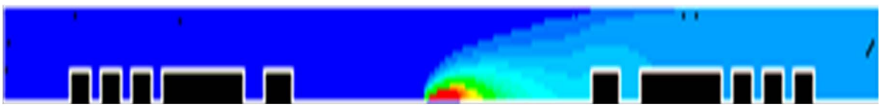

Figure 7. Simulation contour display of dimensionless concentration (K) of CO_2 (wind speed, 0.1 m/s).

The above simulations were performed for the CAMPUS model (path). The contours shows that the intensity of the dispersion depends on the wind speed.

2.3.7. Standard Models Employed

1) The general form of the governing equations:

$$\frac{\partial \rho}{\partial t}+\frac{\partial u_i}{\partial x_i}=0$$

$$\rho\frac{\partial u_i}{\partial t}+\rho\frac{\partial}{\partial x_j}\left(u_j u_i+\overline{u_i' u_j'}\right)=-\frac{\partial P}{\partial x_i}+\frac{\partial}{\partial x_i}\left(\tau_{ij}\right)$$

$$\frac{\partial C^{\alpha}}{\partial t}+u_j\frac{\partial C^{\alpha}}{\partial x_j}=\frac{\partial}{\partial x_j}\left(\left(D^{\alpha}+\frac{\nu_t}{Sc_t}\right)\frac{\partial C^{\alpha}}{\partial x_j}\right)$$

The above equations are respectively; the mass, momentum and species transport of turbulent airflow conservations, which are written in Cartesian tensor notations

in general form. u_i and P are the fluid mean velocity and pressure, u_i' is the fluctuating velocity, ρ represents fluid density. In the species transport Equation, C^α is the concentration of pollutant species α and D^α is its diffusivity, ν_t is the turbulence eddy viscosity, and Sc_t is turbulence Schmidt number.

The term $\rho\overline{u_i'u_j'}$ is the time-averaged rate of momentum transfer due to turbulence. The Reynolds stress tensor $\tau_{ij} = -\overline{u_i'u_j'}$ is given by

$$\overline{u_i'u_j'} = \frac{\mu_t}{\rho}\left(\frac{\partial u_i}{\partial x_j} + \frac{\partial u_j}{\partial x_i}\right) + \frac{2}{3}k\delta_{ij} \tag{17}$$

The turbulent kinetic energy k is defined as half the trace of the Reynolds stress tensor such that

$$k = \frac{1}{2}\sqrt{\overline{u_i u_j}}$$

2) The k-ε model: To determine the turbulent velocity and the length scales, the k-ε model (two equation model) is used that solves one transport equation for turbulent kinetic energy k and another for dissipation rate ε and written as:

$$\rho\frac{Dk}{Dt} = \frac{\partial}{\partial x_j}\left[\left(\mu + \frac{\mu_t}{\sigma_k}\right)\frac{\partial k}{\partial x_j}\right] + \mu_t S^2 - \rho\varepsilon \tag{18}$$

$$\rho\frac{D\varepsilon}{Dt} = \frac{\partial}{\partial x_j}\left[\left(\mu + \frac{\mu_t}{\sigma_\varepsilon}\right)\frac{\partial \varepsilon}{\partial x_j}\right] + \frac{\varepsilon}{k}\left(c_{1\varepsilon}\mu_t S^2 - \rho c_2\varepsilon\right) \tag{19}$$

3) The sstk-ω turbulence models: The sstk-ω model on the other hand, has the capability of addressing some of the deficiencies of the k-ε model by solving the standard k equation but uses specific dissipation rate ω as a length-determining factor and written as

$$\rho\frac{Dk}{Dt} = \tau_{ij}\frac{\partial U_i}{\partial x_j} - \rho\beta^* f_{\beta^*} k\omega + \frac{\partial}{\partial x_j}\left[\left(\mu + \frac{\mu_t}{\sigma_k}\right)\frac{\partial k}{\partial x_j}\right] \tag{20}$$

$$\rho\frac{D\omega}{Dt} = \alpha_\omega\frac{\omega}{k}\tau_{ij}\frac{\partial U_i}{\partial x_j} - \rho\beta^* f_{\beta^*} k\omega^2 + \frac{\partial}{\partial x_j}\left[\left(\mu + \frac{\mu_t}{\sigma_\varepsilon}\right)\frac{\partial \varepsilon}{\partial x_j}\right] \tag{21}$$

$$\mu_t = \rho c_\mu\frac{k^2}{\varepsilon}, \quad \varepsilon = \beta^*\omega k \tag{22}$$

2.4. Calculation Parameters in Fluent [31] [32] [35]-[39]

The principal parameters used in the simulations where carefully selected from literature. The choice of the turbulence model was made based on information gathered from the literature, and others are tested and validated in the course of the study. Table 1 summarizes these parameters.

2.5. Experimental Setup

Measurements on the site were obtained, using the gas tester [KIMO-KIGAZ 700 (060322)]. The tester was set to record concentrations after each point following a click. The values were recorded accordingly and printed at the end of each session. The test was carried out during the morning rush hours between 7:00 am to 9:00 am

and evening rush hours, 5:00 pm to 7:00 pm, for five consecutive days. Values were recorded at points corresponding to those used for the numerical simulations and are tabulated. Each measurement is taken five times for both morning and evening sessions, making ten records per point and the average calculated. While measurements where going on, vehicles plying around the campus were being recorded.

Table 1. Simulation parameters.

DEFINITION		INPUT PARAMETER
Solver		Pressure based
Model		Viscous-k-ε
Material properties		C_p = 29.085 J/mol·K
Boundary conditions	Velocity inlet 2	- Velocity 1.08 m/s - Turbulence kinetic energy 0.004374 m^2/s^2 - Turbulence dissipation rate 0.000042 m^2/s^3
	Velocity inlet 1	- About 1 m/s [19], 0.8 m/s adopted - Turbulence kinetic energy 0.0024 m^2/s^2 - Turbulence dissipation rate 0.000017 m^2/s^3
	- Outflows (default)	
	- Walls (maintain 300˚k for temperatures)	

2.6. Field Measurement

2.6.1. Vehicle CO_2 Emission Calculation

The amount of CO_2 emissions emitted from automotive vehicles, can be calculated using the following formula [6]. Automobiles were not classified by type, therefore average emission factor for small cars, medium cars and large cars are calculated and used.

$$\begin{aligned} \mathrm{CO_2\ emission} = {} & \mathrm{vol}\left(\mathrm{unit/hour}\right) \times \mathrm{streetlength}\left(\mathrm{km}\right) \\ & \times \mathrm{emission\ factor}\left(\mathrm{g\ CO_2/km}\right) \end{aligned} \tag{23}$$

2.6.2. Characteristics of the Studied Area

Changes in the carbon dioxide emission field were investigated in campus A, ie in the main campus of the University of Douala which on the north is facing the busy street from «Ange Raphael» to the Cocoa processing industry known as «SIG Cacao», on the left side is a less busy street to campus B through st. Thomas Aquinas university parish, and also runs behind the campus, on the right is an earth road leading into the neighboring surroundings. Opposite the campus and its surroundings are private buildings for living and commercial activities. The campus covers about (424 m × 172 m) of which large part is occupied by the faculty buildings, classroom blocks, University restaurant, health center, and sporting play ground. The campus comprises 25 buildings of varying sizes, while the surrounding buildings are many and of varying sizes and heights. The configuration of the

campus is shown in Figure 8. The paths (models) are designated with respect to the main University service found on the path, e.g. CAMPUSRESTAU, is named as a result of the fact that the University restaurant building is on the chosen path. Figure 9 shows a top view of the campus outlook, which is measured and designed in AutoCAD software.

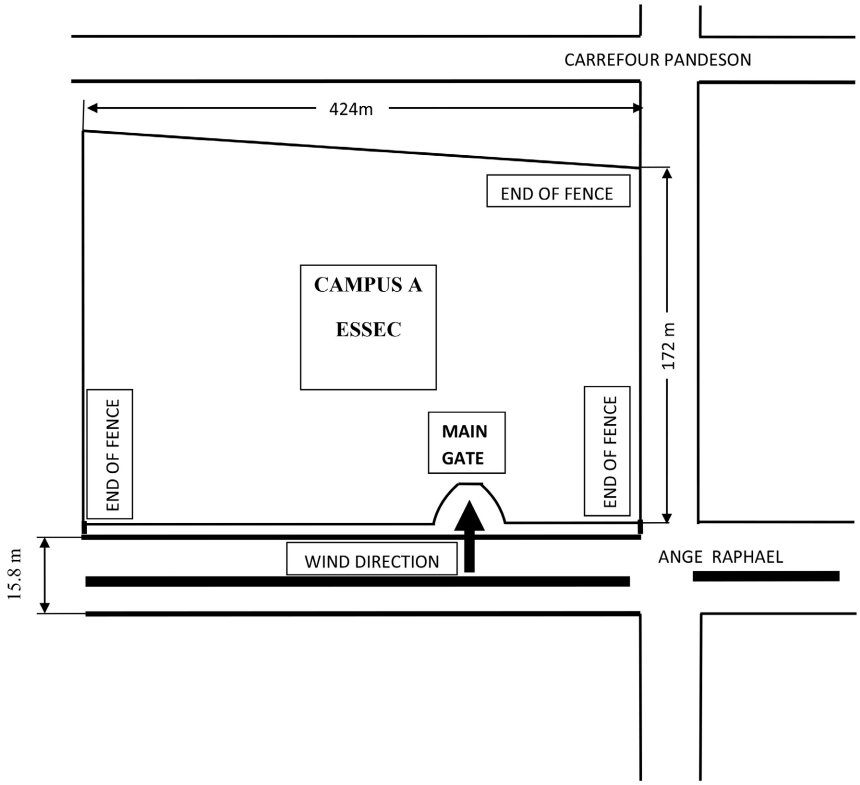

Figure 8. Block diagram of the campus model.

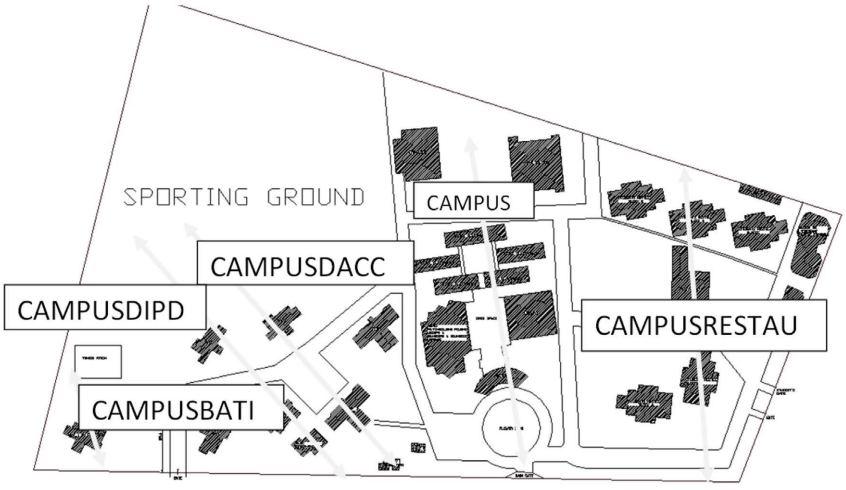

Figure 9. Chosen models (paths) within the campus configuration.

In this study, observations on the series of buildings situated in the main cam-

pus of the University of Douala, will enable to estimate the concentration of CO_2 with the aid of the software Fluent and compare with measured values for five selected paths. The CAMPUS model (path) being the baseline, with a street canyon of 42 walls. Measurements were taken at each wall center. This study was done basing on the following major assumptions:

- The buildings are all of the same height for each path chosen.
- The urban roughness is due to the building disposition and not on the surface roughness of the walls.
- A line source just like in the experiment of Meroney *et al.* [31].
- Wind direction is perpendicular to the buildings, with an average value of about 1.1 m/s.
- Estimations are made on the chosen paths and will be generalized to the entire campus accordingly.

3. Results and Discussion

To investigate the emission and concentration of CO_2 in and around the main campus of the university of Douala, simulations and experiments were designed and run. Results were expressed in the form of characteristic curves and bar charts. The curves present non dimensional concentrations at chosen points on the paths (models). The quantity of emission and concentration of CO_2 is an indicator of the air quality.

1) Results on the concentration of CO_2 for different wind speeds. The combined graph for different velocities of the CAMPUS Model shows that a wind speed of 0.8 m/s agrees most to the experimental result.

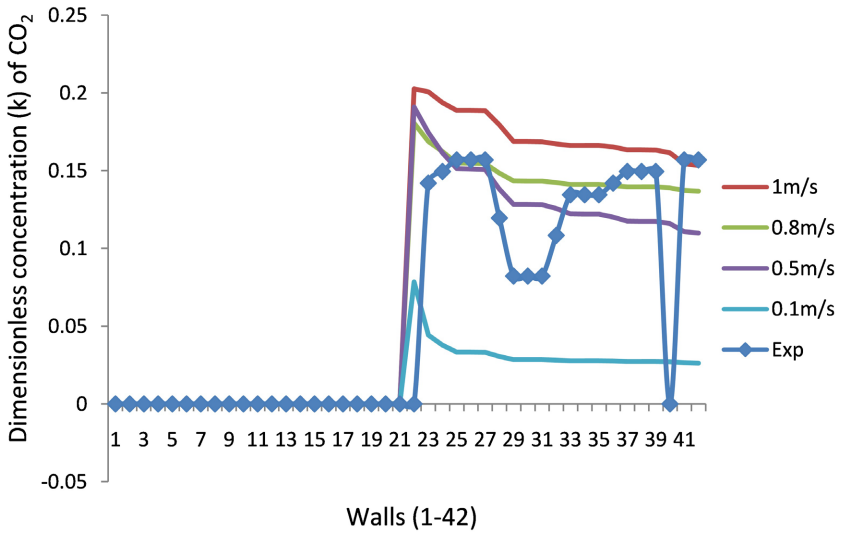

Figure 10. CO_2 Concentrations for different simulated wind speeds and measured values.

The fact that the values of the simulation at various velocities don't match perfectly with experimentation, is due to poor accuracy as a result of the discretization. The number of cells is fewer, to facilitate convergence and avoid computer

space problems. Figure 10. Shows the CO_2 for the different wind speeds and the measured values at the CAMPUS model. Due to the smallest error of 3.8%, between simulated and measured concentrations at a wind speed of 0.8 m/s, this wind speed is then adopted and used for the simulation of the other four models.

2) Validation of results of the concentration CO_2 in the various paths. The plots of the measured and simulated data for the individual paths are shown in Figure 11. The scatter diagram of the measured data shows the tendency of following the pattern of the simulated data. The measured and simulated data is shown in Figure 11(a) for the CAMPUSDACC model, Figure 11(b) for the CAMPUSSRESTAU, Figure 11(c) for the CAMPUSDIPD, and Figure 11(d) for the CAMPUSBATI models. The largest difference in value between the simulated and the measured net concentrations, is observed for the CAMPUSDACC model; 3.14 and O.91 respectively. However, there is an encouraging correlation between the data sets 0.6335, turning towards the lower threshold for good correlations (0.7).

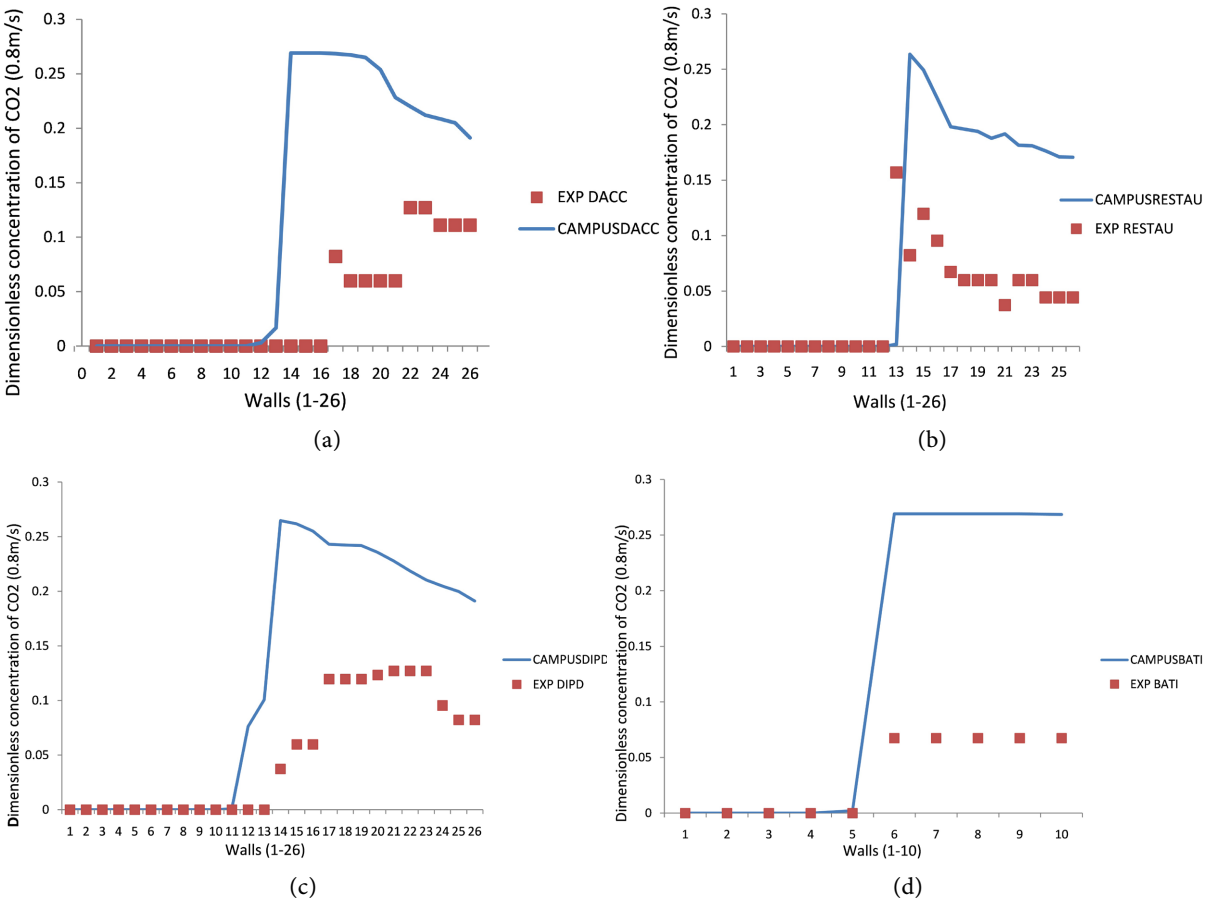

Figure 11. (a) Plot for CAMPUSDACC versus measured CO_2 concentrations; (b) Plot for CAMPUSRESTAU versus measured CO_2 concentrations; (c) Plot for CAMPUSDIPD versus measured CO_2 concentrations; (d) Plot for CAMPUSBATI versus measured CO_2 concentrations.

3) Net simulated and measured concentrations of CO_2. Figure 12 displays the net concentrations on the various street canyon models. The results of the model

entitled CAMPUSDIPD shows a higher concentration of CO_2 (3.17%), and CAMPUS BATI the least (1.35%). The geometry and number of building blocks on both paths, explains why the values are high or low. CAMPUSDIPD, has more building blocks than CAMPUSBATI, which contents the least number of bocks.

Even though, the CAMPUS model has more building blocks than CAMPUDDIPD, simulation still produced a higher concentration for the later. This can be explained by the fact that, k-ε model that was employed, even though it takes less computer space, is not very accurate as SST k-ω, used in the study of Li *et al.* [17].

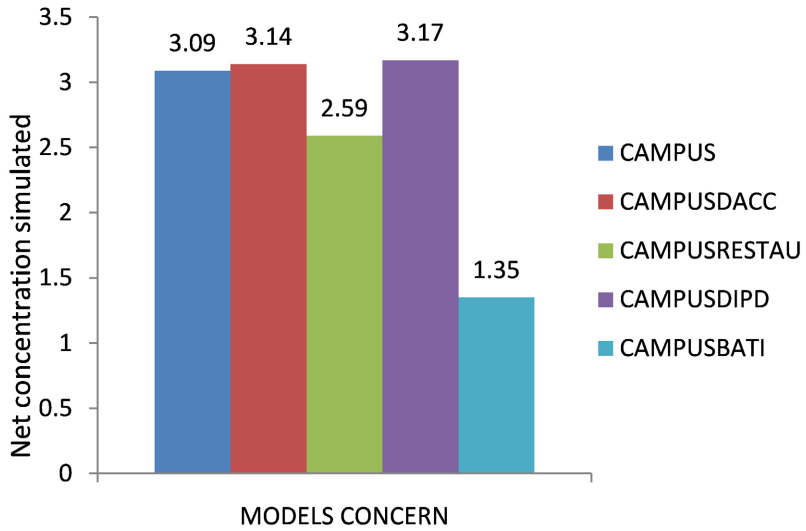

Figure 12. Net simulated concentration of CO_2 for various models.

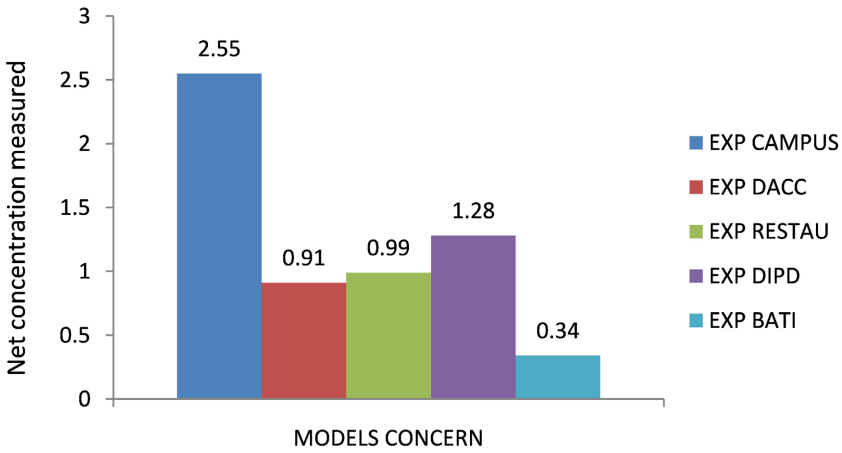

Figure 13. Net measured concentration of CO_2 for the various models.

For the measured values in **Figure 13**, highest value of net concentration is at the CAMPUS Model (2.55%), while the least is still the CAMPUSBATI (0.34%). This sounds realistic, since there are more blocks of building on the path containing CAMPUS model than any of the paths, while CAMPUSBATI has the least number of building blocks.

Fu *et al.* [13] in a study revealed that, canyon geometry strongly influences hu-

man exposure to traffic pollutants in the populated urban area. This supports the fact that paths with large number of buildings could likely suffer from high concentration of pollutants.

4) The Amount of CO_2 Emission from Automobiles Around the Campus

The CO_2 emissions from automobiles are estimated. The CO_2 emissions are calculated based on Equation 23 and the data in Table 2. The emission factor is taken as an average of the values for different classes of automobiles. Other data are calculated here, such as vehicle number, road length. The results of the CO_2 emission calculation are displayed in Table 2. The calculation results show that the highest vehicle emissions are generated by motorcycles at 75.8 kg/2 hours, for a total of 2204 motorcycles. The total CO_2 emissions in the study area are 143.2 kg/2 hours.

The values of CO_2 are expressed per two hours as due to the fact that the average data recorded were for two hours periods corresponding to the morning and evening rush periods. Similar findings were conducted by Aini *et al.* [6], reporting a highest CO_2 emission of 231.6 kg/h, for a total 6814 motorcycles/h. This indicates that, even though the emissions factor for motorcycles is smaller, their very large numbers in cities have a significant effect on the air quality.

Table 2. Average flux of vehicles around the campus during the experiment.

Street concern	Type of automobile	Average rush Hour Traffic (unit/2 hrs)	Length of street (km)	Average emission Factor (Kg CO_2/km)	CO_2 emission (kg/2 h)
Front street	Vehicles (cars, buses, trucks)	710	0.424	0.19132	57.6
	Motorcycles	2,034	0.424	0.08499	73.3
Right side street	Vehicles (cars, buses, trucks)	299	0.172	0.19132	9.8
	Motorcycles	170	0.172	0.08499	2.5
Average total number of vehicles during the experiment	1009			67.4	
Average total number of motorcycles during the experiment	2,204			75.8	
	TOTAL CO_2 emission				143.2

4. Conclusion

In the course of this study, results for the emission and concentration of CO_2 in street canyons were obtained. Paths (models) were chosen, simulations and measurement done. 2-D models were generated from chosen site, CAMPUS A of the University of Douala which permitted us to determine the zone of high CO_2 concentrations. With the increasing number of motorcycles in the cities, air quality will continue to deteriorate. City administrators need to enforce regulations on the use of motorcycles. These will help to curb the rate of emission in cities and free city dwellers from respiratory ill health. The measuring process could be im-

proved upon, by acquiring more equipment adapted to the purpose. The CAMPUS model being the zone with highest concentrations, entails care should be taken by the occupants of the building blocks on that path during rush hours. Clean air policies need to be adopted, particularly in the buildings around this zone and the campus as a whole. More trees could be planted around the University fence to limit the gases reaching the buildings and the occupants. More can be done to valorize studies like this, through the use of an experimental wind tunnel (E.W.T). Furthermore, the study can be extended to other sites in the city of Douala, and to the other pollutants like CO, NOx, to name a few.

Acknowledgements

This work has been successful thanks to the assistance of the following:

- Garage Marine Cameroon, for their enormous contribution to the measurement of CO_2. Providing the measuring instruments.
- Pr KANA Thomas, for his close follow-up of this work. His attachments, guidance, advices and provision of related ideas.

Conflicts of Interest

The authors declare that there is no conflict of interest regarding the publication of this paper.

References

[1] Mori, R. (2018) Air Pollution Mitigation by Urban Greening. *Italus Hortus*, **25**, 13-22. https://doi.org/10.26353/j.itahort/2018.1.1322

[2] (2025) Cameroon: Regions, Major Cities & Towns—Population Statistics, Maps, Charts, Weather and Web Information. https://www.citypopulation.de/en/cameroon/cities

[3] (2021) Volkswagen, Motor Exhaust Emissions, Self-Study Programme 230. https://Procarmanuals.com

[4] Bjorkegren, A.B., Grimmond, C.S.B., Kotthaus, S. and Malamud, B.D. (2015) CO_2 Emission Estimation in the Urban Environment: Measurement of the CO_2 Storage Term. *Atmospheric Environment*, **122**, 775-790. https://doi.org/10.1016/j.atmosenv.2015.10.012

[5] Cichowicz, R. and Wielgosiński, G. (2015) Effect of Urban Traffic on the Immission of Carbon Dioxide in the University Campus. *Ecological Chemistry and Engineering S*, **22**, 189-200. https://doi.org/10.1515/eces-2015-0010

[6] Aini, N., Shen, Z., Wikantiyoso, R., Tutuko, P. and Maksimilianus Gai, A. (2023) Evaluation of the Shape of Tree Crowns to Protect Air Quality on the Roadside from the Co_2 Dispersion Produced by Transportation. *International Review for Spatial Planning and Sustainable Development*, **11**, 26-41. https://doi.org/10.14246/irspsd.11.2_26

[7] Sofia, D., Giuliano, A. and Gioiella, F. (2018) Air Quality Monitoring Network for Tracking Pollutants: The Case Study of Salerno City Center. *Chemical Engineering Transactions*, **68**, 67-72.

[8] Sjöberg, K., Söderlund, K., Swietlicki, E., Kristensson, A. and Krejci, R. (2023) Air

Quality and Swedish Air Quality Monitoring. Swedish Environmental Protection Agency.

[9] Madalozzo, D.M.S., Braun, A.L. and Awruch, A.M. (2012) A Numerical Model for Pollutant Dispersion Simulation in Street Canyons. *Mecánica Computacional*, **XXXI**, 211-235.

[10] Miao, Y., Liu, S., Zheng, Y., Wang, S. and Li, Y. (2014) Numerical Study of Traffic Pollutant Dispersion within Different Street Canyon Configurations. *Advances in Meteorology*, **2014**, Article ID: 458671. https://doi.org/10.1155/2014/458671

[11] Voordeckers, D., Lauriks, T., Denys, S., Billen, P., Tytgat, T. and Van Acker, M. (2021) Guidelines for Passive Control of Traffic-Related Air Pollution in Street Canyons: An Overview for Urban Planning. *Landscape and Urban Planning*, **207**, Article ID: 103980. https://doi.org/10.1016/j.landurbplan.2020.103980

[12] Gartmann, A., Müller, M.D., Parlow, E. and Vogt, R. (2011) Evaluation of Numerical Simulations of CO_2 Transport in a City Block with Field Measurements. *Environmental Fluid Mechanics*, **12**, 185-200. https://doi.org/10.1007/s10652-011-9226-z

[13] Fu, X., Liu, J., Ban-Weiss, G.A., Zhang, J., Huang, X., Ouyang, B., *et al.* (2017) Effects of Canyon Geometry on the Distribution of Traffic-Related Air Pollution in a Large Urban Area: Implications of a Multi-Canyon Air Pollution Dispersion Model. *Atmospheric Environment*, **165**, 111-121. https://doi.org/10.1016/j.atmosenv.2017.06.031

[14] Zhu, X.X., Wang, X.Y., Lei, L. and Zhao, Y.T. (2022) Pollution Dispersion in Urban Street Canyon with Green Belts. *Computer Modelling in Engineering & Science*, **132**, 661-679.

[15] Lo, K.W. and Ngan, K. (2017) Characterizing Ventilation and Exposure in Street Canyons Using Lagrangian Particles. *Journal of Applied Meteorology and Climatology*, **56**, 1177-1194. https://doi.org/10.1175/jamc-d-16-0168.1

[16] Chomcheon, S., Khajohnsaksumeth, N., Wiwatanapataphee, B. and Ge, X. (2019) Modeling and Simulation of Air Pollutant Distribution in Street Canyon Area with Skytrain Stations. *Advances in Difference Equations*, **2019**, Article No. 459. https://doi.org/10.1186/s13662-019-2382-z

[17] Li, C., Liu, L. and Tan, W. (2019) Evaluation of RSM for Simulating Dispersion of CO_2 Cloud in Flat and Urban Terrains. *Aerosol and Air Quality Research*, **19**, 390-398. https://doi.org/10.4209/aaqr.2018.09.0328

[18] Croitoru, C. and Nastase, I. (2018) A State of the Art Regarding Urban Air Quality Prediction Models. *E3S Web of Conferences*, **32**, Article ID: 01010. https://doi.org/10.1051/e3sconf/20183201010

[19] Kwak, K., Woo, S., Kim, K., Lee, S., Bae, G., Ma, Y., *et al.* (2018) On-Road Air Quality Associated with Traffic Composition and Street-Canyon Ventilation: Mobile Monitoring and CFD Modeling. *Atmosphere*, **9**, Article 92. https://doi.org/10.3390/atmos9030092

[20] Lv, W., Wu, Y. and Zang, J. (2021) A Review on the Dispersion and Distribution Characteristics of Pollutants in Street Canyons and Improvement Measures. *Energies*, **14**, Article 6155. https://doi.org/10.3390/en14196155

[21] Ketzel, M., Jensen, S.S., Brandt, J., Ellermann, T., Olesen, H.R., Berkowicz, R. and Hertel, O. (2012) Evaluation of the Street Pollution Model OSPM for Measurements at 12 Streets Stations Using a Newly Developed and Freely Available Evaluation Tool. *Journal of Civil & Environmental Engineering*, **1**, 1-11.

[22] Berkowicz, R., Hertel, O., Larsen, S.E., Sørensen, N.N. and Nielsen, M. (1997) Mod-

elling Traffic Pollution in Streets. National Environmental Research Institute.

[23] Evans, G.J., Audette, C., Badali, K., Celo, V., Dabek-Zlotorszynka, E., Debosz, J., *et al.* (2019) Near-Road Air Pollution Pilot Study Final Report. Southern Ontario Centre for Atmospheric Aerosol Research, University of Toronto.

[24] Gregory, D., Mclaughlin, O., Mullender, S. and Sundararajah, N. (2016) New Solutions to Air Pollution Challenges in the UK. London Forum for Science and Policy Briefing Paper.

[25] King, M.F., Noakes, C.J. and Barlow, J.F. (2015) Urban Pollution and Indoor Air Quality, an Undisputed Relationship: CFD Modelling of Single-Sided Pollutant Ingress. *Healthy Buildings* 2015—*Europe*, Eindhoven, 18-20 May 2015, 5 p.

[26] Taylor, C.F. (1985) The Internal Combustion Engine in Theory and Practice, volume 1. 2nd Edition, The MIT Press, 507.

[27] Plate, E.J. (1982) Wind Tunnel Modelling of Wind Effects in Engineering. *Engineering Meteorology*, **25**, 573-640.

[28] de Nevers, N. (2000) Air pollution Control Engineering. 2nd Edition, Mc Graw Hill.

[29] Price, J.F. (2006) Lagrangian and Eulerian Representations of Fluid Flow: Kinematics and the Equations of Motion. http://www.whoi.edu/science/PO/people/jprice

[30] Patankar, S.V. (1980) Numerical Heat Transfer and Fluid Flow, Series in Computational Methods in Mechanics and Thermal Sciences. Mc Graw-Hill.

[31] Meroney, R.N., Pavageau, M., Rafailidis, S. and Schatzmann, M. (1996) Study of Line Source Characteristics for 2-D Physical Modelling of Pollutant Dispersion in Street Canyons. *Journal of Wind Engineering and Industrial Aerodynamics*, **62**, 37-56. https://doi.org/10.1016/s0167-6105(96)00057-8

[32] Gad, I.A.M., Nasief, M.M., Abdel Aaziz, S.S. and Osman, A.A. (2009) Modeling of Air Pollutant Dispersion in Street Canyons in Cross-Wind. 13*th international Conference on Aerospace Sciences & Aviation Technology*, Cairo, 26-28 May 2009, 1-13. https://doi.org/10.21608/ASAT.2009.23848

[33] Plate, E.J. (1996) Wind Tunnel Modeling of Traffic Induced Pollution in Cities. Institut für Hydrologie und Wasserwirtschaft, universität Karlsruhe, Germany.

[34] Kastner-Klein, P.M. (1996) Wind Tunnel Modeling of Traffic Induced Pollution in Cities, Research Associate. Instiut für Hydrologie und Wasserwirtschaft, universität Karlsruhe, Germany.

[35] (2004) GAMBIT 2.2, Tutorial Guide. http://www.fluent.com/

[36] (2009) Tutorial Gambit. http://thetsis.enscbp.fr

[37] Fluent-ANSYI (2006) Fluent 6.3 Tutorial Guide. Introduction to Using Fluent: Fluid Flow and Heat Transfer in a Mixing Flow, Fluent Inc.

[38] Fluent-ANSYI (2006) Tutorial 13. Modelling Species Transport and Gaseous Combustion, Fluent Inc.

[39] Fluent-ANSYI (2006) Fluent 6.3 User's Guide, Fluent Inc.

Abbreviations

CEMAC: «Communauté Economique et Monitaire de l'Afrique Central»
CFD: Computaional Fluid Dynamic.
EC: Eddy Covariance.
E.W.T: Environmental Wind Tunnel.
F.E.M: Finite Element Methods
HEVs: High Emitting Vehicles.
IAQ: Indoor Air Quality.
LES: Large Eddy Simulation.
OSPM: Operational Street Pollution Model.
PM: Particulate Matter.
RANS: Reynolds Average Navier-Stokes.
RNG: Renormalized Group.
RSM: Reyonds Stress Model.
SST k-ω: Share Stress Transport k-ω.